UC Irvine
Faculty Publications

Title

Phosphate supply explains variation in nucleic acid allocation but not C : P stoichiometry in the western North Atlantic

Permalink

Journal

ISSN

Authors

Zimmerman, A. E
Martiny, A. C
Lomas, M. W
et al.

Publication Date

DOI

Copyright Information

Peer reviewed

Biogeosciences

Phosphate supply explains variation in nucleic acid allocation but not C : P stoichiometry in the western North Atlantic

A. E. Zimmerman[1,3], A. C. Martiny[1,2], M. W. Lomas[4], and S. D. Allison[1,2]

[1]Department of Ecology and Evolutionary Biology, University of California Irvine, Irvine, CA 92697-2525, USA
[2]Department of Earth System Science, University of California Irvine, Irvine, CA 92697-3100, USA
[3]Monterey Bay Aquarium Research Institute, Moss Landing, CA 95039, USA
[4]Bigelow Laboratory for Ocean Sciences, East Boothbay, ME 04544, USA

Correspondence to: A. E. Zimmerman (amyz@mbari.org)

Abstract. Marine microbial communities mediate many biogeochemical transformations in the ocean. Consequently, processes such as primary production and carbon (C) export are linked to nutrient regeneration and are influenced by the resource demand and elemental composition of marine microbial biomass. Laboratory studies have demonstrated that differential partitioning of element resources to various cellular components can directly influence overall cellular elemental ratios, especially with respect to growth machinery (i.e., ribosomal RNA) and phosphorus (P) allocation. To investigate whether allocation to RNA is related to biomass P content and overall C : P biomass composition in the open ocean, we characterized patterns of P allocation and C : P elemental ratios along an environmental gradient of phosphate supply in the North Atlantic subtropical gyre (NASG) from 35.67° N, 64.17° W to 22.676° N, 65.526° W. Because the NASG is characterized as a P-stressed ecosystem, we hypothesized that biochemical allocation would reflect sensitivity to bioavailable phosphate, such that greater phosphate supply would result in increased allocation toward P-rich RNA for growth. We predicted these changes in allocation would also result in lower C : P ratios with increased phosphate supply. However, bulk C : P ratios were decoupled from allocation to nucleic acids and did not appear to vary systematically across a phosphate supply gradient of 2.2–14.7 µmol m^{-2} d^{-1}. Overall, we found that C : P ratios ranged from 188 to 306 along the transect, and RNA represented only 6–12 % of total particulate P, whereas DNA represented 11–19 %. We did find that allocation to RNA was positively correlated with phosphate supply rate, suggesting a consistent physiological response in biochemical allocation to resource supply within the whole community. These results suggest that community composition and/or nonnucleic acid P pools may influence ecosystem-scale variation in C : P stoichiometry more than nucleic acid allocation or P supply in diverse marine microbial communities.

1 Introduction

Redfield observations of the stoichiometric similarly between dissolved nutrients in the deep ocean and surface ocean plankton represent one of the cornerstones of marine biogeochemistry (Redfield, 1934, 1958). Coupling among macronutrients across dissolved and particulate fractions carries consequences for the flux of energy and elements in marine systems (Arrigo, 1999; Deutsch and Weber, 2012; Hessen et al., 2004). For example, carbon (C): phosphorus (P) ratios link nutrient cycling with CO_2 fixation and the biological C pump (Omta et al., 2006; Tyrrell, 1999). It is now clear that broad-scale spatial and temporal variability in elemental ratios and departures from Redfield proportions are common (Martiny et al., 2013; Michaels et al., 2001). Furthermore, incorporating stoichiometric flexibility into ecological models has improved their ability to capture certain biogeochemical dynamics (Christian, 2005; Deutsch and Weber, 2012; Flynn, 2010). Understanding both the patterns and mechanisms of stoichiometric variability is central to interpreting biogeochemical data and predicting ecological consequences.

Several mechanisms have been identified that may contribute to variation in stoichiometric ratios at various scales. Marine plankton have taxon-specific limitations on biomass stoichiometry and can have different stoichiometric composition under the same environmental conditions (Grob et al., 2013; Quigg et al., 2003, 2011; Zimmerman et al., 2013). Consequently, community composition affects community stoichiometry, and may contribute to significant differences between oceanic regions (Martiny et al., 2013; Weber and Deutsch, 2010). Several studies have also demonstrated significant differences in elemental stoichiometry as populations or communities respond to prevailing environmental conditions, most often characterized by nutrient supply ratios (Bratbak, 1985; Rhee, 1978; Tezuka, 1990; Vrede et al., 2002). Taxonomic constraints and nutrient supply are not mutually exclusive mechanisms and likely interact along environmental gradients to influence stoichiometry at ecosystem scales.

Underlying these mechanisms is a dynamic allocation of cellular resources according to ecological growth strategy (Elser et al., 2003; Franklin et al., 2011; Klausmeier et al., 2004; Vrede et al., 2004). Biochemical allocation influences the elemental composition of a cell via inherent elemental differences in biomolecules, including proteins, carbohydrates, nucleic acids, lipids, and polyphosphate (Geider and La Roche, 2002; Sterner and Elser, 2002). Nucleic acids in particular have been highlighted as quantitatively important to cellular P quotas due to their relatively high P content and the necessity of ribosomal RNA (rRNA) for growth (Elser et al., 2000, 2003; Sterner and Elser, 2002). In the field of ecological stoichiometry, relationships among RNA content, biomass P, and growth are formalized as the growth rate hypothesis (GRH). The influence of RNA P on total cellular P content is expected to be strongest under conditions of P limitation (Elser et al., 2003; Makino et al., 2003), implying that differential nucleic acid allocation may significantly contribute to variation in community C : P stoichiometry in P-limited ecosystems. To our knowledge, the relationships between RNA allocation and P content, and the resulting impact on biomass C : P ratios have been studied exclusively in culture-based experiments, and no published studies have examined these relationships in the open ocean.

The Sargasso Sea in the North Atlantic subtropical gyre (NASG) is characterized by low concentrations of dissolved inorganic P and rapid turnover rates, which indicate conditions of P stress (Ammerman et al., 2003; Cavender-Bares et al., 2001; Cotner et al., 1997; Mather et al., 2008; Wu et al., 2000). Evidence suggests that chronic P depletion has driven organisms from the western NASG to evolve sophisticated genetic mechanisms for responding to P fluctuations (Coleman and Chisholm, 2010; Martiny et al., 2006). Plankton can use both dissolved inorganic and organic forms to satisfy cellular P quotas (Casey et al., 2009; Lomas et al., 2010), but inorganic forms (operationally defined as soluble reactive phosphorus, SRP) are more directly bioavailable and

preferred by osmotrophs (Dyhrman et al., 2007; Moore et al., 2005). Accordingly, taxon-specific rates of inorganic P uptake by native plankton responded positively to increasing SRP concentration (Casey et al., 2009). Biochemical allocation may be similarly responsive to SRP supply in the western NASG, but this prediction remains to be tested.

The objective of this study was to analyze the relationship between biochemical allocation strategy and nutrient supply in open ocean communities to evaluate a potential driver of ecosystem-scale variability in the particulate element ratios of surface waters. To address this objective, we analyzed biological pools of P and biomass C : P ratios of bulk seawater along a latitudinal gradient in the Sargasso Sea representing a range of SRP supply rates. The surface waters north of the Bermuda Atlantic Time-series Study (BATS; 31.67° N, 64.17° W) station generally experience more frequent exchange with nutrient-rich deep water due to convective mixing, resulting in higher SRP fluxes at the northern latitudes than in the more permanently stratified water of the southern latitudes (Cavender-Bares et al., 2001). We hypothesized that in this P-depleted system, SRP supply influences biochemical allocation, with increased allocation toward P-rich RNA for growth at higher SRP flux rates. In turn, we hypothesized that these changes in allocation may reduce biomass C : P ratios. We therefore expected higher SRP fluxes to correlate with higher total RNA, RNA : DNA ratios, proportion of P allocated to RNA and total P biomass but lower C : P ratios. Support for our hypothesis would imply that the RNA allocation strategy is a principal biological mechanism for linking nutrient supply to variation in biomass stoichiometry at the ecosystem scale.

2   Methods

2.1   Sample collection

Samples were collected from a Niskin bottle on a rosette equipped with a CTD instrument (conductivity, temperature and depth; Sea-bird Electronics, Inc., Bellevue, WA, USA) during cruise AE1226/BV47 aboard the R/V *Atlantic Explorer* in the Sargasso Sea (Fig. 1). Sampling occurred from 27 September to 6 October 2012 on a transect from 35.67° N, 64.176° W to 22.67° N, 65.52° W, past the BATS site at 31.67° N, 64.17° W (Fig. 1).

Samples were collected for determination of particulate (nominally > 0.3 μm) organic carbon (POC), particulate phosphorus (PPhos), nucleic acids (RNA and DNA), soluble reactive phosphorus (SRP), and total dissolved phosphorus (TDP). Surface seawater (≤ 5 m depth) from replicate Niskin bottles was collected directly into polycarbonate Nalgene bottles (Thermo Scientific Nalgene, Rochester, NY, USA), which had previously been washed with Micro-90 detergent (International Products Corp., Burlington, NJ, USA) and 10 % HCl (with repeated rinsing after each wash), and
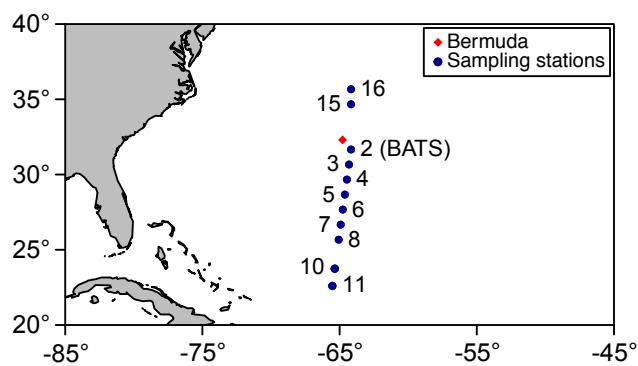
Fig. 1. Map of sampling stations in the North Atlantic subtropical gyre during the BV47 cruise in 2012. The BATS site corresponds to station 2. All samples were collected from surface water (< 10 m).

rinsed three times with the seawater to be sampled. Subsamples from each replicate Nalgene bottle were immediately collected onto precombusted (450 °C, 5 h) 0.3-μm-pore-size glass fiber filters (Sterlitech Corp., Kent, WA, USA) under gentle filtration for POC, PPhos, and nucleic acid concentrations. Filters for nucleic acid analyses were flash frozen in liquid nitrogen and stored at −80 °C for up to 10 days, while filters for POC and PPhos analyses were stored at −20 °C for up to 1 month. Filter blanks (rinsed with high-purity water) were also collected as described and processed identically to the samples. Separate samples for SRP and TDP analyses were collected from different Niskin bottles on the same hydrocasts, representing depths from 0 to 250 m. SRP and TDP samples were stored unfiltered in acid-cleaned, high-density polyethylene (HDPE) bottles at −20 °C until analysis (Lomas et al., 2010).

Additional hydrographic and biogeochemical measurements were collected at each sampling station (st.) and are accessible through the BATS web page (http://bats.bios.edu/). Sample collection and analysis details for these additional parameters can be found in the *BATS Method Manual* (Knap et al., 1997) or online (http://bats.bios.edu/). To complement our data, we analyzed POC, PPhos, and SRP concentrations from three additional cruises in this region but spanning multiple seasons (cruise X0705 in June 2007, BVal39 in October 2007, and X0804 in May 2008). SRP flux and surface C : P ratios were calculated and analyzed as described below.

2.2 Sample analysis

2.2.1 Dissolved phosphorus pools

SRP concentrations were measured using the magnesium-induced co-precipitation method (MAGIC, Karl and Tien, 1992) with modifications as described by Lomas et al. (2010). TDP concentrations were determined using a modified version of the high temperature/acid persulfate

oxidation method (Lomas et al., 2010; Ridal and Moore, 1990). Dissolved organic phosphorus (DOP) concentrations were calculated as the difference between TDP and SRP concentrations. The upward flux of SRP was calculated as the product of the coefficient of vertical diffusivity (0.000035 $m^2\,s^{-1}$ for BATS, Ledwell et al., 2008) and the concentration gradient from 80–160 m at each sampling station. SRP was drawn down to the method detection limit above 80 m, thus SRP flux could not be calculated reliably over shallower depths. For stations where the measured concentration gradient was ambiguous (stations 4, 7, and 10), SRP flux was linearly interpolated from the two immediately adjacent values.

2.2.2 Particulate elements

POC was determined using a CHN analyzer (Thermo Finnigan EA 1112) after samples were treated with HCl (0.2 M) to remove inorganic material and dried overnight at 65 °C. Sample C mass was calculated from chromatogram area using atropine standards and corrected for filter blanks. PPhos was determined using an ash-hydrolysis method with $MgSO_4$ (0.017 M) treatment as previously described (Lomas et al., 2010; Solorzano and Sharp, 1980). Sample P was calculated from a linear regression of absorbance vs. known concentrations of potassium phosphate standards and corrected for filter blanks. PPhos includes both organic and inorganic phosphorus, as no effort was made to separate the two fractions. POC and PPhos bulk concentrations and nutrient molar ratios are reported.

2.2.3 Nucleic acids

Seawater RNA and DNA concentrations were determined using high-sensitivity, macromolecule-specific Quant-iT fluorophores (Molecular Probes, Inc., Eugene, OR, USA) following a crude lysis as previously described (Zimmerman et al., 2013). Briefly, nucleic acids and proteins were released from filters by mechanical lysis (MP FastPrep-24 bead beater, MP Biomedicals, Solon, OH, USA) in a solution of Tris buffer (5 mM) and RNA preservative (saturated ammonium sulfate solution). Sample supernatant was used to prepare assays in 96-well microplates with fluorescent dye, buffer, and prediluted standards provided with each kit (*E. coli* rRNA or λ ds-DNA). Fluorescence was measured on a SpectraMax M2 microplate reader (Molecular Devices, LLC, Sunnyvale, CA). Standards, buffers, and reagents were stored and used according to the manufacturer's suggestions. Spiked control samples from the ship's underway system were included to account for potential signal quench. Macromolecule concentrations were calculated based on standard curve regressions of fluorescence vs. known standard concentrations. The amount of P present in RNA (RNA-P) and DNA (DNA-P) was calculated assuming nucleic acids are 9 % P on average (Sterner and Elser, 2002).
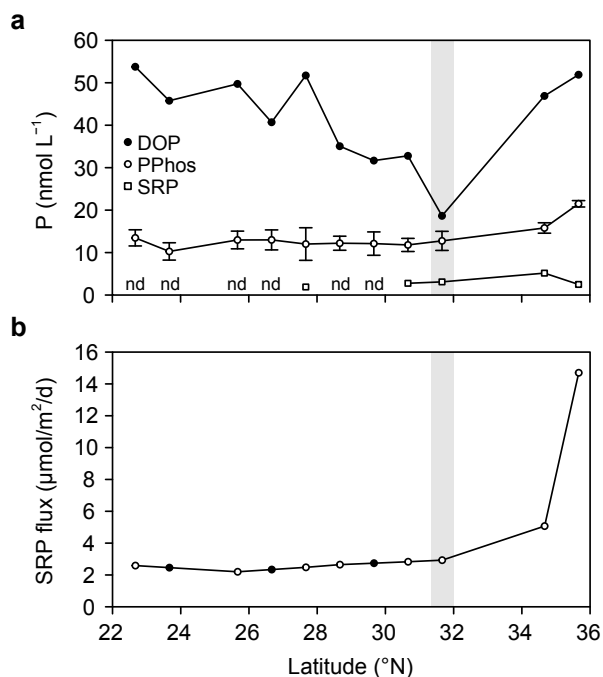
Fig. 2. Phosphorus pools as a function of latitude across the BV47 cruise transect (see Fig. 1). Shaded region represents the approximate location of BATS. **(a)** Surface concentrations of dissolved organic phosphorus (DOP, filled circles), bulk particulate phosphorus (PPhos, open circles; shown as means ± SE), and soluble reactive phosphorus (SRP, open squares, "nd" denotes stations that were below detection). **(b)** Estimated vertical SRP flux (μmol m^{-2} d^{-1}) across the base of the euphotic zone. Flux was calculated as the product of the vertical concentration gradient (from 80 to 160 m) and diffusivity coefficient (0.000035 m^2 s^{-1}; Ledwell et al., 2008). Filled circles represent stations where the SRP flux was linearly interpolated from the two immediately adjacent values because the concentration gradient was not measurable.

2.3 Statistical analysis

All statistical analyses were conducted using the "stats" package in R (R Core Team, 2012). Values are expressed as means ± standard error (SE), unless otherwise indicated. Differences in allocation and stoichiometry among stations along the transect were examined using analysis of variance (ANOVA). Data that did not meet assumptions of normality and homoscedasticity were evaluated with the nonparametric Kruskal–Wallis ANOVA. Spearman's rank correlations were used to assess latitudinal trends, as well as associations between measured variables. This correlation analysis reduces the influence of outlying data points that were observed in our data set (e.g., st. 16 SRP flux). We used Wilcoxon signed rank tests to test whether C : P ratios differed from Redfield proportions (C : P = 106) at each station ($n = 4$ per station) and averaged across all stations ($n = 11$). We also used Wilcoxon signed rank tests to test for differences between RNA and DNA allocation along the transect. We considered all statistical analyses to be significant for P < 0.05.
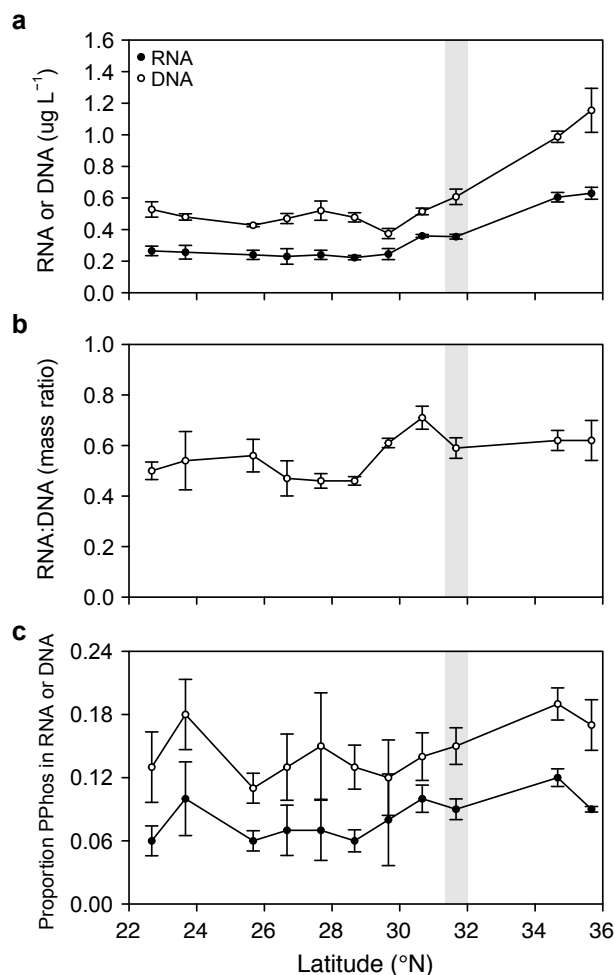

Fig. 3. Allocation to nucleic acids as a function of latitude across the BV47 cruise transect (see Fig. 1). Shaded region represents the approximate location of BATS. All points represent means ± SE. **(a)** Concentrations (μg L^{-1}) of particulate RNA (filled circles) and DNA (open circles). Concentrations of DNA were consistently higher than RNA (P < 0.001, Wilcoxon signed rank test). **(b)** RNA : DNA mass ratios. **(c)** Phosphorus in nucleic acids as a proportion of total particulate phosphorus (PPhos). The proportion of PPhos in RNA was consistently lower than in DNA (P = 0.004, Wilcoxon signed rank test).

3 Results

3.1 Transect description

We analyzed biological allocation of P resources and particulate C : P ratios of bulk seawater at 11 stations along a N–S transect spanning 13° of latitude (22.67–35.67° N; 1445 km) in the oligotrophic Sargasso Sea (Fig. 1; Table 1). Surface (≤ 5 m) water temperature was negatively correlated with latitude (Spearman rank correlation, $\rho = -0.92$, P < 0.001; Fig. A1), and decreased from 28.8 °C at 22.67° N (st. 11) to 25.7 °C north of the BATS station (34.67° N, st. 15).

Table 1. Summary of abiotic and biotic transect parameters[a], including surface concentrations and upward flux of SRP and concentrations of TDP, DOP, PPhos, POC, and nucleic acids (RNA and DNA). Particulate C : P molar ratios and proportions of total PPhos in RNA and DNA (P_{RNA} and P_{DNA}) were also calculated.

Station	Latitude (° N)	SRP flux[b] ($\mu mol\,m^{-2}\,d^{-1}$)	TDP ($nmol\,L^{-1}$)	SRP[c] ($nmol\,L^{-1}$)	DOP ($nmol\,L^{-1}$)	PPhos ($nmol\,L^{-1}$)	POC ($\mu mol\,L^{-1}$)	C : P	RNA ($\mu g\,L^{-1}$)	DNA ($\mu g\,L^{-1}$)	RNA: DNA	P_{RNA}	P_{DNA}
11	22.67	2.59	54.3	NA	53.8	13.5	3.6	264	0.27	0.53	0.50	0.06	0.13
10	23.67	2.46	46.3	NA	45.8	10.3	2.8	291	0.26	0.48	0.54	0.10	0.18
8	25.67	2.20	50.2	NA	49.7	13.0	2.4	189	0.24	0.43	0.56	0.06	0.11
7	26.67	2.34	41.2	NA	40.7	13.0	2.8	229	0.23	0.47	0.47	0.07	0.13
6	27.67	2.48	53.6	1.9	51.7	12.0	2.7	242	0.24	0.52	0.46	0.07	0.15
5	28.67	2.65	35.6	NA	35.1	12.2	3.9	306	0.22	0.48	0.46	0.06	0.13
4	29.67	2.74	32.2	NA	31.7	12.1	2.4	210	0.25	0.38	0.61	0.08	0.12
3	30.67	2.83	35.6	2.8	32.8	11.8	3.0	257	0.36	0.52	0.71	0.10	0.14
2	31.66	2.93	21.8	3.1	18.7	12.8	3.0	244	0.36	0.61	0.59	0.09	0.15
15	34.67	5.07	52.1	5.2	46.9	15.8	3.9	242	0.61	0.99	0.62	0.12	0.19
16	35.67	14.70	54.4	2.5	51.9	21.5	4.1	188	0.63	1.16	0.62	0.09	0.17

[a] Values shown represent the mean of four station replicates, except for TDP, SRP, and DOP ($n = 2$). Geometric means are reported for the C : P ratios. [b] SRP flux values for stations 4, 7, and 10 were calculated from linear interpolation of the two immediately adjacent stations. [c] NA, value was below detection.

Consequently, variation in temperature is inherent to the latitudinal trends described below.

3.2 Latitudinal trends in phosphorus pools

DOP was the largest P pool measured, ranging from 18.7 to 53.8 $nmol\,L^{-1}$ (Fig. 2a), but was not significantly correlated with latitude. The highest DOP concentrations were found at either end of the transect, with the lowest concentration occurring at the BATS station. All of the surface SRP concentrations were low ($< 5\,nmol\,L^{-1}$; Fig. 2a), and six stations were below the nominal detection limit of the MAGIC-SRP method ($\sim 1\,nmol\,L^{-1}$; Lomas et al., 2010). Mean PPhos concentrations varied only by a factor of 2 among stations, with the variation across stations marginally significant ($P = 0.052$, ANOVA; Fig. 2a). The highest PPhos concentration ($21.5\,nmol\,L^{-1}$) was found at the northernmost station ($35.67° N$, st. 16). The lowest concentration of PPhos ($10.3\,nmol\,L^{-1}$) occurred at $23.67° N$ (st. 10, Fig. 2a), but was still twofold higher than the maximum SRP concentration. Estimated vertical SRP flux across the base of the euphotic zone (80–160 m) ranged from 2.2 $\mu mol\,m^{-2}\,d^{-1}$ at $25.67° N$ (st. 8) up to 14.7 $\mu mol\,m^{-2}\,d^{-1}$ at $35.67° N$ (st. 16; Fig. 2b). This diapycnal SRP flux was relatively consistent in the lower- and mid-latitudes of the transect, but showed a distinct increase north of BATS, as would be expected near the edge of the Gulf Stream. SRP flux was significantly correlated with latitude (Spearman rank correlation, $\rho = 0.88$, $P < 0.001$). Bulk POC varied significantly among stations ($P = 0.002$, Kruskal–Wallis ANOVA; Fig. A2), but did not show a directional change with increasing latitude (Spearman rank correlation, $\rho = 0.46$, $P = 0.082$).

3.3 Latitudinal trends in nucleic acids

Concentrations of bulk particulate RNA and DNA in surface waters varied $\sim$ threefold across stations ($P < 0.001$ for both, ANOVA; Fig. 3a), ranging 0.22–0.63 $\mu g\,L^{-1}$ for RNA and

0.38–1.15 $\mu g\,L^{-1}$ for DNA. Similar to SRP flux, both nucleic acids showed relatively uniform concentrations in the lower latitudes and an increase at the north end of the transect (Spearman rank correlations, RNA : $\rho = 0.59$, $P = 0.027$, DNA: $\rho = 0.51$, $P = 0.057$). Concentrations of DNA were consistently higher than RNA ($P < 0.001$, Wilcoxon signed rank test), and RNA : DNA ratios along the transect varied significantly from 0.46 to 0.71 ($P = 0.046$, ANOVA; Fig. 3b). In contrast to total nucleic acid concentrations, the maximum RNA : DNA ratio was at $30.67° N$ (st. 3), just south of BATS, but RNA : DNA ratios across stations still showed a significant monotonic increase with latitude (Spearman rank correlation, $\rho = 0.65$, $P = 0.016$). Overall, the contribution of P in nucleic acids to total PPhos was low ($< 32\%$ in RNA and DNA combined; Fig. 3c), and the proportion of PPhos in RNA (P_{RNA}, 0.06–0.12) was lower than in DNA (P_{DNA}, 0.11–0.19; $P = 0.004$, Wilcoxon signed rank test). Allocation of P to both nucleic acids was variable and did not significantly differ among stations, but mean P_{RNA} was positively correlated with latitude across the transect (Spearman rank correlation, $\rho = 0.57$, $P = 0.034$).

3.4 Latitudinal trends in C : P stoichiometry

Particulate C : P ratios were significantly greater than Redfield (C : P = 106) at all stations ($P < 0.001$, Wilcoxon signed rank test), ranging from 188 to 306, but showed no significant trend with latitude (Fig. 4a). Plotting POC against PPhos revealed a significant positive relationship (Spearman rank correlation, $\rho = 0.56$, $P = 0.038$; Fig. 4b).

3.5 Response to gradients in nutrient flux

Contrary to our expectation, bulk PPhos concentrations did not significantly increase with SRP flux across sampling stations (Spearman rank correlation, $\rho = 0.33$, $P = 0.164$; Fig. 5). Furthermore, we did not find total PPhos concentrations to be significantly dependent on RNA-P (Spearman rank
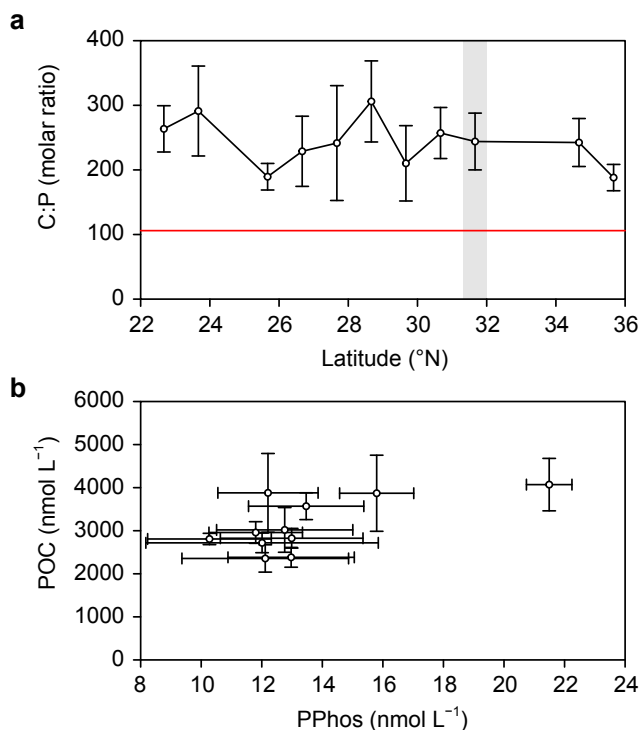
Fig. 5. PPhos as a function of vertical flux of SRP across the BV47 transect (see Fig. 1). Points represent means ± SE. PPhos was not significantly correlated with SRP flux (Spearman rank correlation, $\rho = 0.33$, P = 0.164).

Fig. 4. Relationships between POC and PPhos among sampling stations. **(a)** C : P molar ratio (geometric means ± SE) as a function of latitude across the BV47 transect (see Fig. 1). Shaded region represents approximate location of BATS. C : P ratios were greater than Redfield (C : P = 106, red line) at all stations (P < 0.001, Wilcoxon signed rank test). **(b)** POC as a function of PPhos (Spearman rank correlation, $\rho = 0.56$, P = 0.038). Points represent means ± SE.

correlation, $\rho = 0.35$, P = 0.150; Fig. A3). By comparison, bulk particulate RNA and DNA concentrations both significantly increased with the SRP supply rate along the transect (Spearman rank correlations, RNA : $\rho = 0.77$, P = 0.003, DNA : $\rho = 0.69$, P = 0.012; Fig. 6a). Similar relationships with SRP flux were observed for RNA : DNA ratios (Spearman rank correlations, $\rho = 0.66$, P = 0.013; Fig. 6b), as well as the proportion of PPhos in RNA or DNA (Spearman rank correlations, RNA : $\rho = 0.57$, P = 0.034, DNA: $\rho = 0.51$, P = 0.054; Fig. 6c).

Overall, whole community C : P ratios were not significantly related to SRP flux for our 2012 samples (Spearman rank correlation, $\rho = -0.06$, P = 0.441; Fig. 7) or for previous transects through the same region (Fig. A4). The relationship between POC and SRP flux, however, was significant for our samples (Spearman rank correlation, $\rho = 0.63$, P = 0.022; Fig. A5).

4 Discussion

We hypothesized that greater supply of phosphate across the base of the euphotic zone in the northern latitudes of the Sargasso Sea would s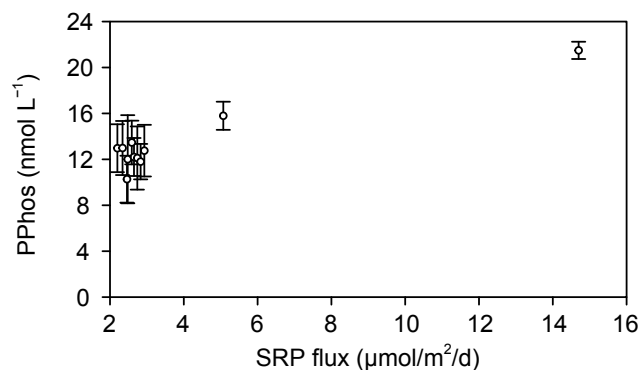upport more P biomass and facilitate greater biochemical allocation toward P-rich RNA for growth than in the more permanently stratified lower latitudes. Phosphate supply (operationally defined as soluble reactive phosphorus, SRP) varied sevenfold across our latitudinal transect (Fig. 2b, Table 1), but this gradient was accompanied by less variation in biochemical allocation (1.5-fold for RNA : DNA ratio, threefold for nucleic acid concentration) in corresponding surface waters (Fig. 3, Table 1). In support of our hypothesis, we found evidence for a community-level increase in allocation to RNA in response to higher SRP supply rates (Fig. 6); however, a concurrent increase in total PPhos with SRP flux was not supported (Fig. 5). This disconnect may reflect a mismatch in sampling horizons, although previous studies in this region clearly show that phytoplankton in the surface mixed layer obtain nutrients from depth (Fawcett et al., 2011, 2014; Johnson et al., 2010). Therefore it is likely that phosphate from depth supports surface plankton. Alternatively, the relatively small proportion of total PPhos represented by RNA and weak change in RNA : DNA ratio across sampling stations (Table 1) may have contributed to the disconnect between SRP flux and total PPhos.

We additionally predicted that the supply of phosphate from depth is related to community-level C : P stoichiometry in the P-depleted surface waters of the NASG. However, the C : P ratio did not vary systematically with latitude or SRP supply rate (Figs. 4a, 7). Accumulated dead plankton material could mask the effect of changes in the RNA content of living plankton biomass on particulate P content and community C : P ratios. However, this does not appear to be the case in the subtropical North Atlantic, as shown by an analysis of the summed contributions of flow-cytometrically sorted populations to total particulate carbon, nitrogen, and phosphorus pools (Martiny et al., 2013). Thus there was little support for a consistent influence of nutrient supply rate or biochemical allocation on whole community C : P stoichiometry despite a regionally coherent response in biochemical allocation to nutrient supply rate.
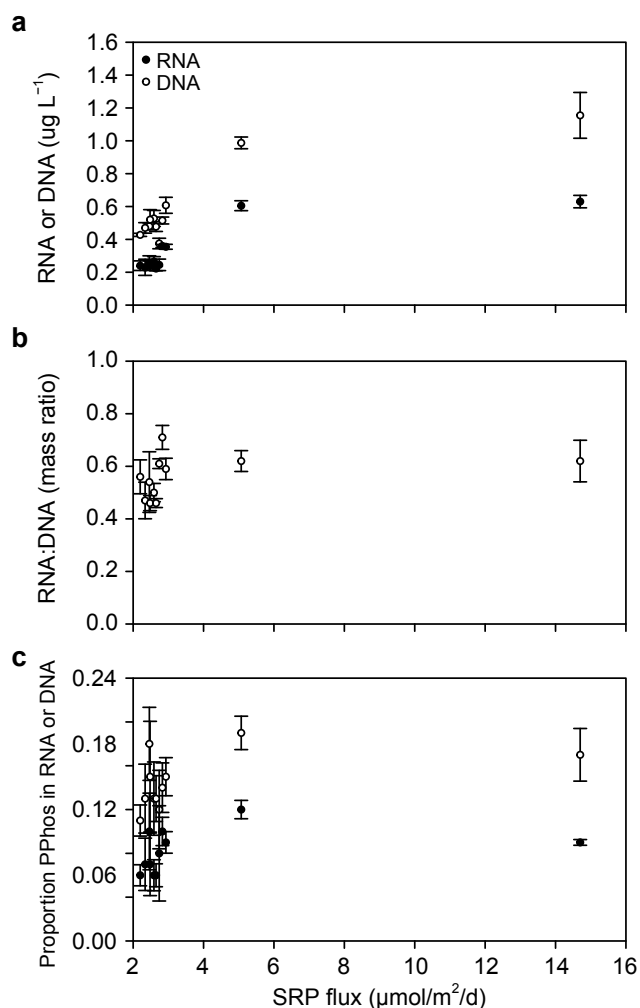
Fig. 6. Allocation to nucleic acids as a function of vertical flux of SRP across the BV47 transect (see Fig. 1). All points represent means ± SE. All measurements of nucleic acids were significantly correlated with SRP supply (Spearman rank correlations). **(a)** Concentrations ($\mu g\,L^{-1}$) of particulate RNA (filled circles, $\rho = 0.77$, $P = 0.003$) and DNA (open circles, $\rho = 0.69$, $P = 0.012$). **(b)** RNA : DNA mass ratios ($\rho = 0.66$, $P = 0.013$). **(c)** The proportion of total PPhos bound in RNA ($\rho = 0.57$, $P = 0.034$) or DNA ($\rho = 0.51$, $P = 0.054$).

Fig. 7. C : P molar ratio as a function of vertical flux of SRP across the BV47 transect (see Fig. 1). Points represent geometric means ± SE. Red line represents Redfield C : P ratio (106). No significant relationship was detected between the C : P ratio and SRP supply ($P = 0.441$)

Both POC and DNA concentrations increased with SRP flux along the transect (Figs. 6a, A5). These results suggest that greater supply of resources from nutrient-rich deep water facilitated an increase in the total biomass supported in surface water. Likewise, the significant increase in the RNA : DNA ratio, a potential proxy for growth rate (Dortch et al., 1983), with SRP supply (Fig. 6b) suggests that community growth rate could be similarly sensitive to nutrient supply. However, we recognize that the correlation between the RNA : DNA ratio and growth rate tends to be weaker for a mixed community than an individual taxon (Jeffrey et al., 1996; Kemp et al., 1993). Though we are unable to tease
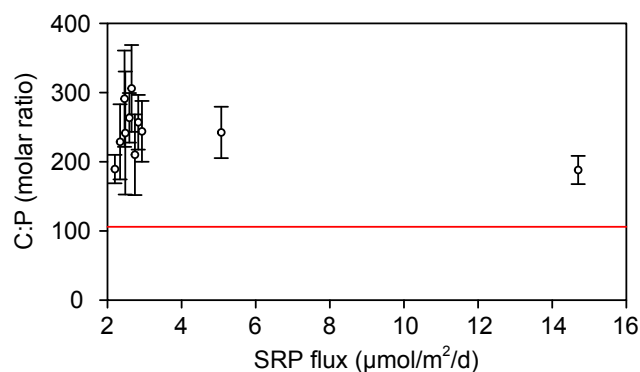
apart the individual influences of SRP and other nutrients that may have been supplied concurrently, high C : P ratios (i.e., significantly greater than Redfield) measured along the transect indicated P stress. Given that the western NASG is characterized by conditions of P stress (Ammerman et al., 2003; Cavender-Bares et al., 2001; Cotner et al., 1997; Mather et al., 2008; Wu et al., 2000), we hypothesize that it is likely P regulates growth and biomass accumulation, though other factors may also have an impact. Higher biomass may be the result of increased carrying capacity of the ecosystem (i.e., greater abundance of individual populations) or a shift to larger cells, whose relatively higher cellular quotas could be supported by the increased supply rate (Chisholm, 1992; Edwards et al., 2012; Marañón et al., 2013). Additionally, with the data we collected, we cannot exclude the possibility that this pattern reflects accumulation of particulate matter resulting from a decrease in loss processes (e.g., grazing and viral lysis).

Although we focused on SRP supply rates under the assumption that SRP is the form of P preferred by marine microbes (Casey et al., 2009), DOP is also important for sustaining primary productivity in the Sargasso Sea (Lomas et al., 2010). DOP may be especially important as an alternative P source at lower SRP supply rates, though we did not detect any significant correlations between DOP and the biological parameters we measured. There does not appear to be long-range transport of DOP from the eastern North Atlantic upwelling regions (Roussenov et al., 2006; Torres-Valdés et al., 2009). Additionally, uptake of SRP by organisms in this region has been shown to be sensitive to SRP concentration while DOP uptake rates were not sensitive to DOP concentration (Casey et al., 2009).

Overall, P from nucleic acids only represented ∼ 22 % of total PPhos (Fig. 3c). Our values are likely driven by generally low concentrations of total particulate RNA and DNA in our samples (Fig. 3a), which correspond to the low end

of values reported for the range of nucleic acid concentrations in the Gulf of Mexico (Jeffrey et al., 1996) and the oligotrophic Mediterranean Sea (Dell'Anno et al., 1999). We recognize that there may be uncertainty in our P_{RNA} and P_{DNA} data because we could not account for potential variation in nucleic acid extraction efficiency due to incomplete cell lysis, and therefore these values should be considered as minimum quotas. Regardless, our calculations of P_{RNA} in natural marine microbial communities are low in comparison to previous studies. Makino et al. (2003) demonstrated that the allocation of P resources to RNA can vary in cultures of *E. coli* from 40 to 80 %, depending on growth rate. Likewise, the proportion of biomass P represented by RNA varied from 25 to 93 % for communities of lake bacteria under manipulated growth and substrate ratio conditions (Makino and Cotner, 2004). In addition to PPhos bound in nucleic acids, ~ 23 % of total PPhos may be found in phospholipids (Van Mooy et al., 2006). Our results suggest that there appear to be additional quantitatively important reservoirs of PPhos for plankton communities in the NASG. A likely candidate is polyphosphate, which has recently also been shown to be part of a stress response to P deficiency in diatoms (Dyhrman et al., 2012) and to increase in concentration from the coastal to open ocean (Martin and Van Mooy, 2013). These potentially important alternative reservoirs of PPhos warrant further investigation in order to comprehensively understand dynamic P allocation in natural plankton communities.

We speculate that taxonomic diversity within communities of marine plankton likely contributed to variation in C : P stoichiometry along the SRP supply gradient. Previous studies have demonstrated that a broad range of plankton taxa, from heterotrophic bacteria to diatoms and micrograzers, persist in this oligotrophic region (DuRand et al., 2001; Longnecker et al., 2010; Treusch et al., 2012; Worden and Binder, 2003), and that the relative abundances of planktonic groups change with latitude (Cavender-Bares et al., 2001; Martiny et al., 2013). These broad taxonomic groups represent a range of ecological and trophic strategies, which inherently differ in resource requirements and may therefore experience varying degrees of P stress in the same environment (Casey et al., 2009; Lomas et al., 2004). For example, photosynthetic machinery imposes different constraints on cellular resource allocation and stoichiometry for autotrophs versus heterotrophs (Vrede et al., 2004). Cell sizes vary across taxonomic groups and are robustly correlated with nutrient uptake and use properties (Chisholm, 1992; Edwards et al., 2012; Marañón et al., 2013). Consequently, multiple effects of broad taxonomic diversity likely interact at the ecosystem scale to constrain emergent community patterns in biochemical allocation and stoichiometry.

Underlying broad-scale taxonomic diversity is additional fine-scale functional diversity in resource use and physiological plasticity related to P cycling. This diversity potentially further exacerbated the decoupling of SRP supply from community C : P stoichiometry in our study. For example, within the well-studied *Prochlorococcus* and *Synechococcus* genera, lineages vary in their P-stress response mechanisms as well as in their ability to use a variety of inorganic and organic P sources (Martiny et al., 2006; Moore et al., 2005). *Synechococcus* also shows interstrain differences in the ability to store P as polyphosphate under conditions of P starvation (Mazard et al., 2012), with probable impacts on cellular C : P ratios. Therefore, different individuals within the same taxonomic group may experience different degrees of P stress and exhibit different strategies when responding to changes in nutrient supply. Accordingly, it may be necessary to evaluate genotype- and even cell-specific responses to environmental P supply to understand variability in the aggregate community patterns of biochemical allocation and stoichiometry in response to large-scale changes in nutrient conditions in the ocean.

Our results have important implications for ecosystem-scale variability in the particulate element ratios of the ocean surface. We have shown that community C : P stoichiometry varied little across a latitudinal gradient of SRP supply (Figs. 4a, 7). PPhos concentrations across the range of the transect were likewise decoupled from both SRP supply rate (Fig. 5) and allocation of biomass P to RNA (Fig. A3). By contrast, we detected a coherent community response in nucleic acid allocation to SRP flux (Fig. 6). Collectively, our results imply that neither biochemical allocation (at least to nucleic acids) nor prevailing environmental conditions (i.e., phosphate supply rate) are the primary mechanisms for explaining emergent community variation in C : P stoichiometry at this scale. We speculate that alternative reservoirs of cellular P, such as phospholipids and storage compounds, and taxonomic composition, which appears to be important at broader spatial scales (Martiny et al., 2013; Weber and Deutsch, 2010), may also constrain ecosystem-scale variation in elemental ratios, though these remain to be tested. Detailed characterization of taxon-specific resource strategies in marine plankton will be essential for identifying the level of taxonomic grouping relevant to understanding emergent community variation in C : P stoichiometry. Building such a framework will in turn strengthen predictions of community response to large-scale changes in ocean nutrient conditions.

References

Ammerman, J. W., Hood, R. R., Case, D. A., and Cotner, J. B.: Phosphorus deficiency in the Atlantic: An emerging paradigm in oceanography, Eos, 84, 165–170, 2003.

Arrigo, K. R.: Phytoplankton community structure and the drawdown of nutrients and CO_2 in the Southern Ocean, Science, 283, 365–367, doi:10.1126/science.283.5400.365, 1999.

Bratbak, G.: Bacterial biovolume and biomass estimations, Appl. Environ. Microbiol., 49, 1488–93, 1985.

Casey, J. R., Lomas, M. W., Michelou, V. K., Dyhrman, S. T., Orchard, E. D., Ammerman, J. W., and Sylvan, J. B.: Phytoplankton taxon-specific orthophosphate (P_i) and ATP utilization in the western subtropical North Atlantic, Aquat. Microb. Ecol., 58, 31–44, doi:10.3354/ame01348, 2009.

Cavender-Bares, K. K., Karl, D. M., and Chisholm, S. W.: Nutrient gradients in the western North Atlantic Ocean: Relationship to microbial community structure and comparison to patterns in the Pacific Ocean, Deep Sea Res.-Pt. I, 48, 2373–2395, doi:10.1016/S0967-0637(01)00027-9, 2001.

Chisholm, S. W.: Phytoplankton size, in: Primary Productivity and Biogeochemical Cycles in the Sea, edited by: Falkowski, P. G. and Woodhead, A. D., Plenum Press, New York, 213–237, 1992.

Christian, J. R.: Biogeochemical cycling in the oligotrophic ocean: Redfield and non-Redfield models, Limnol. Oceanogr., 50, 646–657, 2005.

Coleman, M. L. and Chisholm, S. W.: Ecosystem-specific selection pressures revealed through comparative population genomics, P. Natl. Acad. Sci. USA, 107, 18634–18639, doi:10.1073/pnas.1009480107, 2010.

Cotner, J. B., Ammerman, J. W., Peele, E. R., and Bentzen, E.: Phosphorus-limited bacterioplankton growth in the Sargasso Sea, Aquat. Microb. Ecol., 13, 141–149, 1997.

Dell'Anno, A., Marrale, D., Pusceddu, A., Fabiano, M., and Danovaro, R.: Particulate nucleic acid dynamics in a highly oligotrophic system: The Cretan Sea (Eastern Mediterranean), Mar. Ecol. Prog. Ser., 186, 19–30, 1999.

Deutsch, C. and Weber, T. S.: Nutrient ratios as a tracer and driver of ocean biogeochemistry, Annu. Rev. Mar. Sci., 4, 113–141, 2012.

Dortch, Q., Roberts, T. L., Clayton Jr., J. R., and Ahmed, S. I.: RNA/DNA ratios and DNA concentrations as indicators of growth rate and biomass in planktonic marine organisms, Mar. Ecol. Prog. Ser., 13, 61–71, 1983.

DuRand, M. D., Olson, R. J., and Chisholm, S. W.: Phytoplankton population dynamics at the Bermuda Atlantic Time-series station in the Sargasso Sea, Deep Sea Res.-Pt. II, 48, 1983–2003, doi:10.1016/S0967-0645(00)00166-1, 2001.

Dyhrman, S. T., Ammerman, J. W., and Van Mooy, B. A. S.: Microbes and the marine phosphorus cycle, Oceanography, 20, 110–116, 2007.

Dyhrman, S. T., Jenkins, B. D., Rynearson, T. A., Saito, M. A., Mercier, M. L., Alexander, H., Whitney, L. P., Drzewianowski, A., Bulygin, V. V, Bertrand, E. M., Wu, Z., Benitez-Nelson, C., and Heithoff, A.: The transcriptome and proteome of the diatom Thalassiosira pseudonana reveal a diverse phosphorus stress response, PLoS One, 7, e33768, doi:10.1371/journal.pone.0033768, 2012.

Edwards, K. F., Thomas, M. K., Klausmeier, C. A., and Litchman, E.: Allometric scaling and taxonomic variation in nutrient utilization traits and maximum growth rate of phytoplankton, Limnol. Oceanogr., 57, 554–566, doi:10.4319/lo.2012.57.2.0554, 2012.

Elser, J. J., Sterner, R. W., Gorokhova, E., Fagan, W. F., Markow, T. A., Cotner, J. B., Harrison, J. F., Hobbie, S. E., Odell, G. M., and Weider, L. J.: Biological stoichiometry from genes to ecosystems, Ecol. Lett., 3, 540–550, doi:10.1046/j.1461-0248.2000.00185.x, 2000.

Elser, J. J., Acharya, K., Kyle, M., Cotner, J. B., Makino, W., Markow, T., Watts, T., Hobbie, S. E., Fagan, W., Schade, J., Hood, J. and Sterner, R. W.: Growth rate-stoichiometry couplings in diverse biota, Ecol. Lett., 6, 936–943, doi:10.1046/j.1461-0248.2003.00518.x, 2003.

Fawcett, S. E., Lomas, M. W., Casey, J. R., Ward, B. B., and Sigman, D. M.: Assimilation of upwelled nitrate by small eukaryotes in the Sargasso Sea, Nat. Geosci., 4, 717–722, doi:10.1038/ngeo1265, 2011.

Fawcett, S. E., Lomas, M. W., Ward, B. B., and Sigman, D. M.: The counterintuitive effect of summer-to-fall mixed layer deepening on eukaryotic new production in the Sargasso Sea, Global Biogeochem. Cy., online first, doi:10.1002/2013GB004579, 2014.

Flynn, K. J.: Ecological modelling in a sea of variable stoichiometry: Dysfunctionality and the legacy of Redfield and Monod, Prog. Oceanogr., 84, 52–65, doi:10.1016/j.pocean.2009.09.006, 2010.

Franklin, O., Hall, E. K., Kaiser, C., Battin, T. J., and Richter, A.: Optimization of biomass composition explains microbial growth-stoichiometry relationships, Am. Nat., 177, E29–42, doi:10.1086/657684, 2011.

Geider, R. J. and La Roche, J.: Redfield revisited: variability of C : N : P in marine microalgae and its biochemical basis, Eur. J. Phycol., 37, 1–17, doi:10.1017/S0967026201003456, 2002.

Grob, C., Ostrowski, M., Holland, R. J., Heldal, M., Norland, S., Erichsen, E. S., Blindauer, C., Martin, A. P., Zubkov, M. V., and Scanlan, D. J.: Elemental composition of natural populations of key microbial groups in Atlantic waters, Environ. Microbiol., 15, 3054–3064, doi:10.1111/1462-2920.12145, 2013.

Hessen, D. O., Ågren, G. I., Anderson, T. R., Elser, J. J., and de Ruiter, P. C.: Carbon sequestration in ecosystems: The role of stoichiometry, Ecology, 85, 1179–1192, 2004.

Jeffrey, W. H., Von Haven, R., Hoch, M. P., and Coffin, R. B.: Bacterioplankton RNA, DNA, protein content and relationships to rates of thymidine and leucine incorporation, Aquat. Microb. Ecol., 10, 87–95, 1996.

Johnson, K. S., Riser, S. C., and Karl, D. M.: Nitrate supply from deep to near-surface waters of the North Pacific subtropical gyre, Nature, 465, 1062–1065, doi:10.1038/nature09170, 2010.

Karl, D. M. and Tien, G.: MAGIC: A sensitive and precise method for measuring dissolved phosphorus in aquatic environments, Limnol. Oceanogr., 37, 105–116, doi:10.4319/lo.1992.37.1.0105, 1992.

Kemp, P. F., Lee, S., and Laroche, J.: Estimating the growth rate of slowly growing marine bacteria from RNA content, Appl. Environ. Microbiol., 59, 2594–601, 1993.

Klausmeier, C. A., Litchman, E., Daufresne, T., and Levin, S. A.: Optimal nitrogen-to-phosphorus stoichiometry of phytoplankton, Nature, 429, 171–174, doi:1.1029/2001GL014649, 2004.

Knap, A. H., Michaels, A. F., Steinberg, D. K., Bahr, F., Bates, N., Bell, S., Countway, P., Close, A., Doyle, A., Howse, F., Gundersen, K., Johnson, R., Little, R., Orcutt, K., Parsons, R., Rathbun,

C., Sanderson, M., and Stone, S.: BATS Methods Manual Version 4, available at: http://bats.bios.edu/ (last access: 24 March 2014), 1997.

Ledwell, J. R., McGillicuddy, D. J., and Anderson, L. A.: Nutrient flux into an intense deep chlorophyll layer in a mode-water eddy, Deep Sea Res.-Pt. II, 55, 1139–1160, doi:10.1016/j.dsr2.2008.02.005, 2008.

Lomas, M. W., Swain, A., Shelton, R., and Ammerman, J. W.: Taxonomic variability of phosphorus stress in Sargasso Sea phytoplankton, Limnol. Oceanogr., 49, 2303–2310, 2004.

Lomas, M. W., Burke, A. L., Lomas, D. A., Bell, D. W., Shen, C., Dyhrman, S. T., and Ammerman, J. W.: Sargasso Sea phosphorus biogeochemistry: an important role for dissolved organic phosphorus (DOP), Biogeosciences, 7, 695–710, doi:10.5194/bg-7-695-2010, 2010.

Longnecker, K., Lomas, M. W., and Van Mooy, B. A. S.: Abundance and diversity of heterotrophic bacterial cells assimilating phosphate in the subtropical North Atlantic Ocean, Environ. Microbiol., 12, 2773–2782, doi:10.1111/j.1462-2920.2010.02247.x, 2010.

Makino, W. and Cotner, J. B.: Elemental stoichiometry of a heterotrophic bacterial community in a freshwater lake: Implications for growth- and resource-dependent variations, Aquat. Microb. Ecol., 34, 33–41, doi:10.3354/ame034033, 2004.

Makino, W., Cotner, J. B., Sterner, R. W., and Elser, J. J.: Are bacteria more like plants or animals? Growth rate and resource dependence of bacterial C : N : P stoichiometry, Funct. Ecol., 17, 121–130, doi:10.1046/j.1365-2435.2003.00712.x, 2003.

Marañón, E., Cermeño, P., Lopez-Sandoval, D. C., Rodriguez-Ramos, T., Sobrino, C., Huete-Ortega, M., Blanco, J. M., and Rodriguez, J.: Unimodal size scaling of phytoplankton growth and the size dependence of nutrient uptake and use, Ecol. Lett., 16, 371–379, doi:10.1111/ele.12052, 2013.

Martin, P. and Van Mooy, B. A. S.: Fluorometric quantification of polyphosphate in environmental plankton samples: Extraction protocols, matrix effects, and nucleic acid interference, Appl. Environ. Microbiol., 79, 273–81, doi:10.1128/AEM.02592-12, 2013.

Martiny, A. C., Coleman, M. L., and Chisholm, S. W.: Phosphate acquisition genes in Prochlorococcus ecotypes: Evidence for genome-wide adaptation, P. Natl. Acad. Sci. USA, 103, 12552–12557, doi:10.1073/pnas.0601301103, 2006.

Martiny, A. C., Pham, C. T. A., Primeau, F. W., Vrugt, J. A., Moore, J. K., Levin, S. A., and Lomas, M. W.: Strong latitudinal patterns in the elemental ratios of marine plankton and organic matter, Nat. Geosci., 6, 279–283, doi:10.1038/ngeo1757, 2013.

Mather, R. L., Reynolds, S. E., Wolff, G. A., Williams, R. G., Torres-Valdes, S., Woodward, E. M. S., Landolfi, A., Pan, X., Sanders, R., and Achterberg, E. P.: Phosphorus cycling in the North and South Atlantic Ocean subtropical gyres, Nat. Geosci., 1, 439–443, doi:10.1038/ngeo232, 2008.

Mazard, S., Wilson, W. H., and Scanlan, D. J.: Dissecting the physiological response to phosphorus stress in marine Synechococcus isolates (Cyanophyceae), J. Phycol., 48, 94–105, doi:10.1111/j.1529-8817.2011.01089.x, 2012.

Michaels, A. F., Karl, D. M., and Capone, D. G.: Element stoichiometry, new production and nitrogen fixation, Oceanography, 14, 68–77, doi:10.5670/oceanog.2001.08, 2001.

Moore, L. R., Ostrowski, M., Scanlan, D. J., Feren, K., and Sweetsir, T.: Ecotypic variation in phosphorus-acquisition mechanisms within marine picocyanobacteria, Aquat. Microb. Ecol., 39, 257–269, doi:10.3354/ame039257, 2005.

Omta, A. W., Bruggeman, J., Kooijman, S. A. L. M., and Dijkstra, H. A.: Biological carbon pump revisited: Feedback mechanisms between climate and the Redfield ratio, Geophys. Res. Lett., 33, L14613, doi:10.1029/2006GL026213, 2006.

Quigg, A., Finkel, Z. V, Irwin, A. J., Rosenthal, Y., Ho, T.-Y., Reinfelder, J. R., Schofield, O., Morel, F. M. M., and Falkowski, P. G.: The evolutionary inheritance of elemental stoichiometry in marine phytoplankton, Nature, 425, 291–294, doi:10.1038/nature01953, 2003.

Quigg, A., Irwin, A. J., and Finkel, Z. V: Evolutionary inheritance of elemental stoichiometry in phytoplankton, Proc. R. Soc. B Biol. Sci., 278, 526–534, doi:10.1098/rspb.2010.1356, 2011.

R Core Team: R: A language and environment for statistical computing, R Foundation for Statistical Computing, available at: http://www.r-project.org/ (last access: 24 March 2014), 2012.

Redfield, A. C.: On the proportions of organic derivatives in sea water and their relation to the composition of plankton, in: James Johnstone Memorial Volume, edited by: Daniel, R. J., University Press of Liverpool, 177–192, 1934.

Redfield, A. C.: The biological control of chemical factors in the environment, Am. Sci., 46, 205–221, 1958.

Rhee, G.-Y.: Effects of N : P atomic ratios and nitrate limitation on algal growth, cell composition, nitrate uptake, Limnol. Oceanogr., 23, 10–25, doi:10.4319/lo.1978.23.1.0010, 1978.

Ridal, J. J. and Moore, R. M.: A re-examination of the measurement of dissolved organic phosphorus in seawater, Mar. Chem., 29, 19–31, 1990.

Roussenov, V., Williams, R. G., Mahaffey, C., and Wolff, G. A.: Does the transport of dissolved organic nutrients affect export production in the Atlantic Ocean?, Global Biogeochem. Cy., 20, GB3002, doi:10.1029/2005GB002510, 2006.

Solorzano, L. and Sharp, J. H.: Determination of total dissolved phosphorus and particulate phosphorus in natural water, Limnol. Oceanogr., 25, 754–758, 1980.

Sterner, R. W. and Elser, J. J.: Ecological stoichiometry: The biology of elements from molecules to the biosphere, Princeton University Press, Princeton, 2002.

Tezuka, Y.: Bacterial regeneration of ammonium and phosphate as affected by the carbon:nitrogen:phosphorus ratio of organic substrates, Microb. Ecol., 19, 227–238, doi:10.1007/BF02017167, 1990.

Torres-Valdés, S., Roussenov, V. M., Sanders, R., Reynolds, S., Pan, X., Mather, R., Landolfi, A., Wolff, G. A., Achterberg, E. P., and Williams, R. G.: Distribution of dissolved organic nutrients and their effect on export production over the Atlantic Ocean, Global Biogeochem. Cy., 23, GB4019, doi:10.1029/2008GB003389, 2009.

Treusch, A. H., Demir-Hilton, E., Vergin, K. L., Worden, A. Z., Carlson, C. A., Donatz, M. G., Burton, R. M., and Giovannoni, S. J.: Phytoplankton distribution patterns in the northwestern Sargasso Sea revealed by small subunit rRNA genes from plastids, ISME J., 6, 481–492, doi:10.1038/ismej.2011.117, 2012.

Tyrrell, T.: The relative influences of nitrogen and phosphorus on oceanic primary production, Nature, 400, 525–531, 1999.

Van Mooy, B. A. S., Rocap, G., Fredricks, H. F., Evans, C. T., and Devol, A. H.: Sulfolipids dramatically decrease phosphorus demand by picocyanobacteria in oligotrophic marine environments, P. Natl. Acad. Sci. USA, 103, 8607–8612, doi:10.1073/pnas.0600540103, 2006.

Vrede, K., Heldal, M., Norland, S., and Bratbak, G.: Elemental composition (C, N, P) and cell volume of exponentially growing and nutrient-limited bacterioplankton, Appl. Environ. Microbiol., 68, 2965, doi:10.1128/AEM.68.6.2965, 2002.

Vrede, T., Dobberfuhl, D. R., Kooijman, S. A. L. M., and Elser, J. J.: Fundamental connections among organism C : N : P stoichiometry, macromolecular composition, and growth, Ecology, 85, 1217–1229, 2004.

Weber, T. S. and Deutsch, C.: Ocean nutrient ratios governed by plankton biogeography, Nature, 467, 550–554, doi:10.1038/nature09403, 2010.

Worden, A. Z. and Binder, B. J.: Application of dilution experiments for measuring growth and mortality rates among Prochlorococcus and Synechococcus populations in oligotrophic environments, Aquat. Microb. Ecol., 30, 159–174, doi:10.3354/ame030159, 2003.

Wu, J., Sunda, W., Boyle, E. A., and Karl, D. M.: Phosphate depletion in the Western North Atlantic Ocean, Science, 289, 759–762, doi:10.1126/science.289.5480.759, 2000.

Zimmerman, A. E., Allison, S. D., and Martiny, A. C.: Phylogenetic constraints on elemental stoichiometry and resource allocation in heterotrophic marine bacteria, Environ. Microbiol., online first, doi:10.1111/1462-2920.12329, 2013.

Appendix A
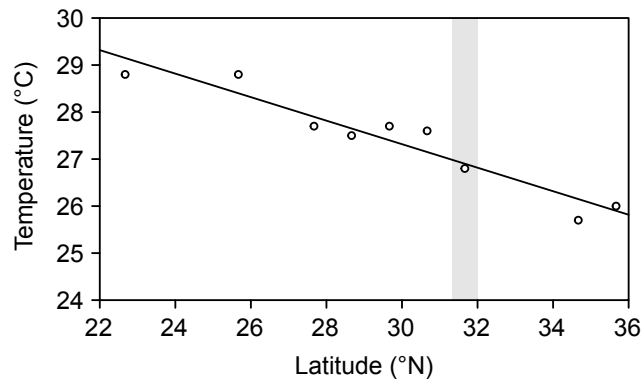
Supplemental figures

Fig. A1. Temperature as a function of latitude across the BV47 cruise transect (see Fig. 1). Shaded region represents approximate location of BATS. Regression line depicts significant inverse relationship between temperature and latitude (Spearman rank correlation, $\rho = -0.92$, $P < 0.001$).
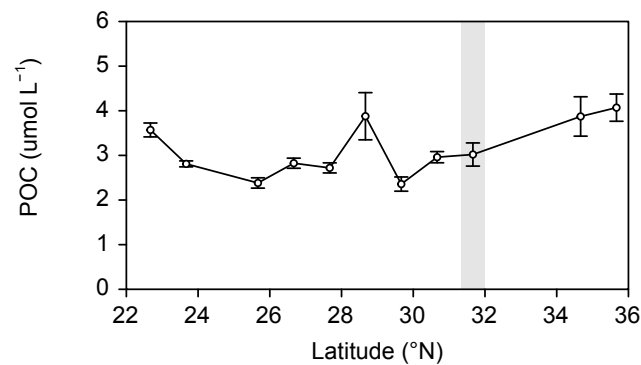

Fig. A2. Particulate organic carbon (POC) as a function of latitude across the BV47 cruise transect (see Fig. 1). Shaded region represents approximate location of BATS. POC varied among stations ($P = 0.002$, Kruskal–Wallis ANOVA – analysis of variance), but was not significantly correlated with latitude (Spearman rank correlation, $\rho = 0.46$, $P = 0.082$).
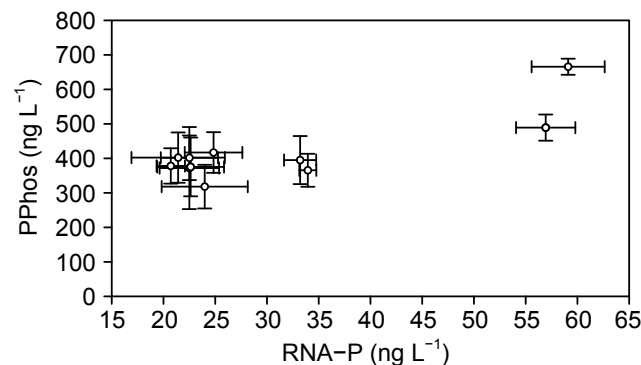

Fig. A3. Particulate phosphorus (PPhos) as a function of phosphorus in RNA (RNA-P, calculated as 9 % RNA mass). Total PPhos was not significantly correlated with RNA-P (Spearman rank correlation, $\rho = 0.35$, $P = 0.150$).
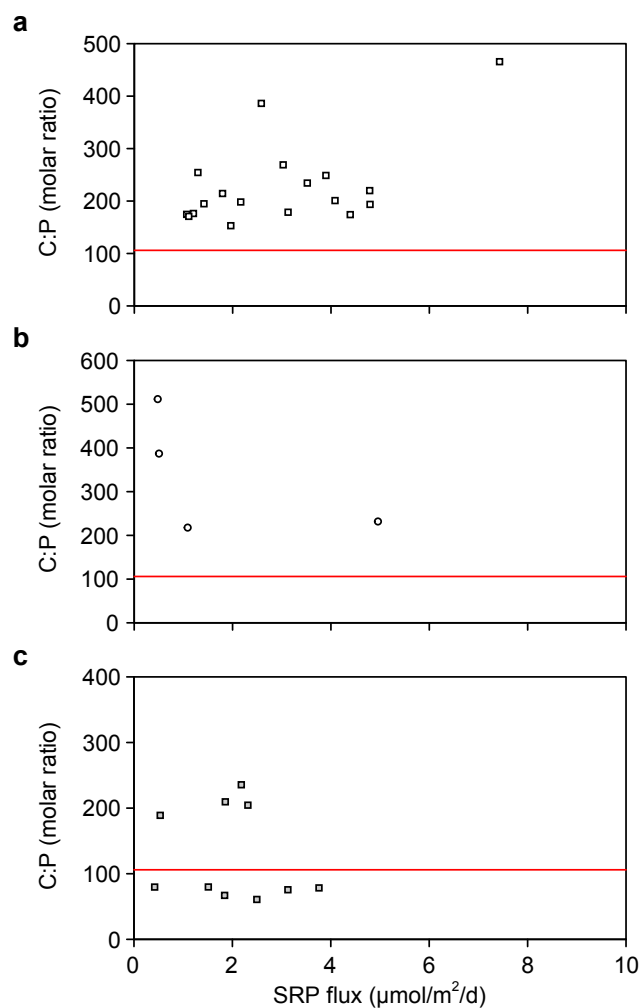
Fig. A4. C : P molar ratio as a function of vertical flux of soluble reactive phosphorus (SRP) from additional cruises in this region across multiple seasons. No significant relationship was detected between C : P ratio and SRP supply (Spearman rank correlations, P > 0.05) for cruise **(a)** X0705 in June 2007 (open squares), **(b)** BVal39 in October 2007 (open circles), or **(c)** X0804 in May 2008 (shaded squares). Data for BVal39 were retrieved from the BATS web page (http://bats.bios.edu/) and data for X0705 and X0804 were retrieved from BCO-DMO (http://www.bco-dmo.org). Red line represents Redfield C : P ratio (106).
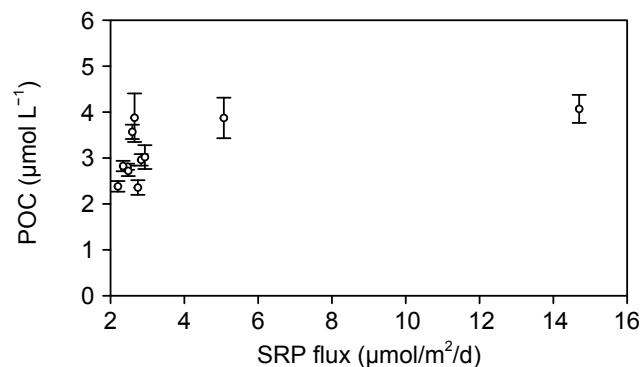

Fig. A5. POC as a function of vertical flux of SRP across the BV47 transect (see Fig. 1). Points represent means ± SE. POC was significantly correlated with SRP flux (Spearman rank correlation, $\rho = 0.63$, P = 0.022).